

Clustering Behaviour in Al-Mg-Si Alloys Investigated by APT

Malin Torsæter¹, Williams Lefebvre², Sigmund J. Andersen³, Calin D. Marioara³, John C. Walmsley^{1,3} and Randi Holmestad¹

¹ Dept. of Physics, Norwegian University of Science and Technology (NTNU), 7491 Trondheim, Norway

² Groupe de Physique des Matériaux, Université de Rouen, 76801 St. Etienne du Rouvray, Cedex, France

³SINTEF Materials and Chemistry, 7465 Trondheim, Norway

Atom Probe Tomography (APT) has been applied to investigate nanometer sized clusters of solute atoms forming in Si-rich alloys of the Al-Mg-Si system. The clusters produced during 2 months of natural ageing in alloys of high and low solute content were investigated and these were compared to the clusters forming during direct pre-ageing treatment. The method used for cluster identification in the APT datasets was the maximum separation algorithm, employing heuristically determined input parameters. Our results showed that clusters with an Mg/Si ratio close to 1 were forming during pre-ageing treatment, and these are assumed to be favourable structures that can easily evolve into more developed phases. The clusters forming during natural ageing in the alloy of low solute content (Mg + Si < 1 wt%) were found to be of the same type as the pre-ageing clusters, explaining why these alloys show a positive effect of room temperature storage. In the naturally aged alloy of high solute content (Mg + Si > 1 wt%), on the other hand, the clusters formed with a broad range of compositions. It is likely that a significant proportion of these can not nucleate hardening precipitates, thereby explaining the negative effect of room temperature storage for these alloys.

Keywords: Al-Mg-Si alloys, clustering, atom probe tomography, natural ageing, pre-ageing.

1. Introduction

Due to properties like high strength-to-weight ratio, good formability and resistance against corrosion, the Al-Mg-Si (6xxx) alloys are widely used for industrial applications. They are heat-treatable alloys showing a large increase in strength upon ageing. This effect is due to the strain created by small, semi-coherent, meta-stable precipitates that form from solid solution. The precipitates constitute a sequence of different structures [1] before they end up in the equilibrium β -Mg₂Si phase, and each type may influence the material properties differently. Strong structural similarities are observed with the precipitates [2], indicating that they are nucleated from similar clusters. Knowledge of the early stages of precipitation can, thereby, reveal information on how the meta-stable phases grow and further evolve.

The early stages of precipitation can be examined by investigating clusters that are believed to be the nuclei of hardening phases. Since pre-ageing treatments of 70°C to 120°C directly after quench are reported to have a positive effect on the material strength, it is likely that such early stage precipitate nuclei are formed in this temperature interval [3, 4].

A hardness increase during room temperature storage is reported for Al-Mg-Si alloys. This is believed to be due to the formation of solute clusters in the matrix, a phenomenon termed *natural ageing* (NA) [5]. As opposed to clusters forming during pre-ageing treatment, the NA clusters are not all believed to act as nuclei for hardening phases. Alloys of solute content higher than about 1 wt% are reported to form “bad” clusters during NA [6]. These have a detrimental effect on subsequent precipitation during artificial ageing, leading to the formation of a lower number density of coarser precipitates that give lower peak hardness than if NA had been avoided [3]. On the other hand, alloys of a lower solute content are reported to form “good” clusters during NA which result in a higher alloy strength when compared to immediate artificial ageing after direct quenching [7].

The present study aims to quantify the early stages of precipitation by investigating the clusters formed during a pre-ageing treatment at 100°C. These precipitate nuclei are further compared to the unfavourable and favourable clusters forming during 2 months of natural ageing in alloys of high and low solute content, respectively. Atom Probe Tomography (APT), which is a well-established method for investigating Al-based alloys [8], was used for collecting experimental data. This was processed by applying the maximum separation method [9], with heuristically determined input parameters, to extract information on clustered atoms.

2. Experimental

All investigated Al-Mg-Si alloys had an Mg/Si ratio lower than 1. The compositions are listed in Table 1. It can be seen that the naturally aged samples producing “bad” clusters (BC) and “good” clusters (GC) originate from industrial alloys, as opposed to the pre-aged sample (PA) that was produced from an ultra-pure alloy. All samples were first solution heat treated for 1 hour at 540°C and further water quenched to room temperature. Subsequently, sample PA was directly pre-aged for 16 hours at 100°C, while samples BC and GC were naturally aged for 2 months before APT experiments.

Samples for APT were prepared by the two-step electropolishing procedure. From thin rods (with a cross section of $0.3 \times 0.3 \text{ mm}^2$) they were polished, initially in 25 % perchloric acid with 75 % acetic acid, and further in a solution of 2 % perchloric acid in 2-butoxyethanol. The instrument used for APT analyses was an energy compensated tomographic atom probe (ECoTAP) [10], equipped with an advanced delay line detector [11]. The experiment was carried out under ultra high vacuum ($\sim 10^{-8}$ Pa), at a temperature of 40 K. This has earlier been demonstrated to be sufficiently low for aluminium alloys [12]. The pulse fraction was set to 20 % and a pulse repetition rate of 1,7 kHz was used. Data processing was performed using software developed at the University of Rouen.

Table 1: Nominal composition, heat treatment history, and collected APT volumes of the three alloy conditions. The directly pre-aged sample is denoted PA while BC and GC are naturally aged, producing “bad” clusters and “good” clusters, respectively.

Sample designation	Heat treatment	Nominal Composition				APT volumes	
		Mg (at%)	Si (at%)	Mn (at%)	Fe (at%)	No. of atoms	Size (nm ³)
PA	16 h at 100°C	0.4	0.84	-	-	441 996	16 140
BC	2 months at RT	0.83	0.91	0.03	0.10	301 340	11 393
GC	2 months at RT	0.41	0.43	0.03	0.10	666 217	27 724

2.1 Cluster identification procedure

In this work the maximum separation method [9] is used for cluster identification. It is based on the principle that solute atoms in clusters are statistically closer together than those that are spread out in the matrix. All solute atoms that are separated from each other by no more than a specified distance d_{max} are assigned to a group. A group is a cluster if its number of solute atoms is equal to, or exceeds, a certain minimum number N_{min} of solute atoms. Even if d_{max} and N_{min} are user-defined input parameters, they greatly influence the outcome of the analysis [13].

To ensure quantitative and comparable results, the two parameters were chosen so as to optimize discrimination between real clusters and random aggregation of solute. This was achieved by applying the maximum separation algorithm both to experimental datasets and to corresponding randomized versions. Randomization in this case means assigning all the measured mass-to-charge ratios for the ions randomly to the set of observed positions, yielding a model of a random solid solution. This enabled the definition of a noise-per-cluster ratio, denoting the number of noise clusters (i.e. clusters identified in the randomized volume) per cluster identified in the experimental dataset. The variations of this quantity as a function of d_{max} and N_{min} for the BC and GC alloy are shown in Figure 1 (a) and (b), respectively.

A successful choice of parameters is a compromise between a low noise-per-cluster ratio (meaning that the clusters identified have a high probability of corresponding to real features in the microstructure), a high number of clusters and a low N_{min} value (enabling the identification of small clusters).

For the alloy low in solute (GC), this heuristic approach led to the parameter choices $d_{max} = 7 \text{ \AA}$ and $N_{min} = 8$. A lower d_{max} value than this, or a higher N_{min} , led to a strong decrease in the number of clusters observed. As seen from Figure 1 (b) the noise-per-cluster graph increases steeply for this alloy, which means that depending on the choice of parameters, the clusters are either completely real (noise-per-cluster = 0.0) or mixed with a lot of noise clusters. For the alloys higher in solute (PA and BC) the distances between solute atoms were overall smaller in the randomized dataset. As seen from Figure 1 (a), it was necessary to decrease the d_{max} parameter to 6 \AA for these alloys to obtain similar noise-per-cluster values. All clusters were thereby ensured to have approximately the same significance above noise level before comparison.

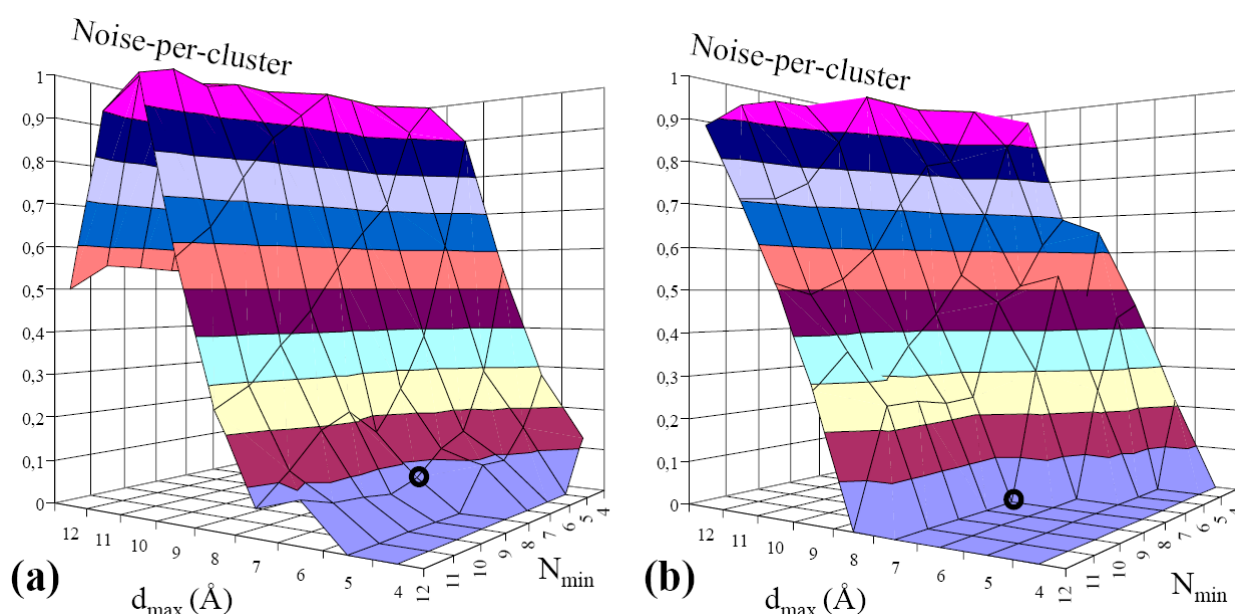


Fig. 1: The variation in the noise-per-cluster ratio as a function of cluster identification parameters for (a) BC: naturally aged sample of high solute content, (b) GC: naturally aged sample of low solute content. The black circles denote the parameters chosen in this work.

3. Results and Discussion

3.1 Cluster number density as obtained by APT

The quantities listed in Table 2 describe the datasets containing clustered solute atoms as obtained by applying the maximum separation method to the alloy conditions listed in Table 1. As seen from their similar noise-per-cluster ratios, the clusters obtained have approximately the same significance; being 90%-100% certain to reflect true features of the alloy microstructure. A visualization of the clusters is given in Figure 2, showing small comparable sections of the large APT volumes that were used for analysis.

The naturally aged sample of high solute content (BC) has the highest number density of clusters and the highest fraction of solute elements contained in clusters (clustered solute atoms / total number of solute atoms). However, naturally aged samples of this alloy are reported to produce a low number density of coarse precipitates upon subsequent artificial ageing [3, 4]. This makes it likely that most of the clusters formed during natural ageing can not act as nucleation sites for hardening precipitates. The high number of competing nuclei correlates well with the reported sluggish precipitation during artificial ageing in naturally aged samples of this alloy [6].

The clusters formed in both the GC and the PA alloys are reported to have a positive effect on subsequent precipitation during ageing. Therefore, it can be assumed that most clusters seen in Figure 2 (a) and (c) contribute to nucleation of more developed precipitates.

Table 2: Characteristic values describing the datasets containing clustered solute atoms as obtained using the maximum separation method on the volumes from Table 1 with parameters $d_{max} = 7 \text{ \AA}$ and $N_{min} = 8$ for GC, and $d_{max} = 6 \text{ \AA}$ and $N_{min} = 8$ for BC and PA.

	PA	BC	GC
Noise-per-cluster	0.10	0.07	0.00
No. of clusters identified	44	39	12
Number density of clusters ($10^6/\mu\text{m}^3$)	2.72	3.42	0.43
Atomic fraction of solute in clusters (%)	6.9	12.2	2.07

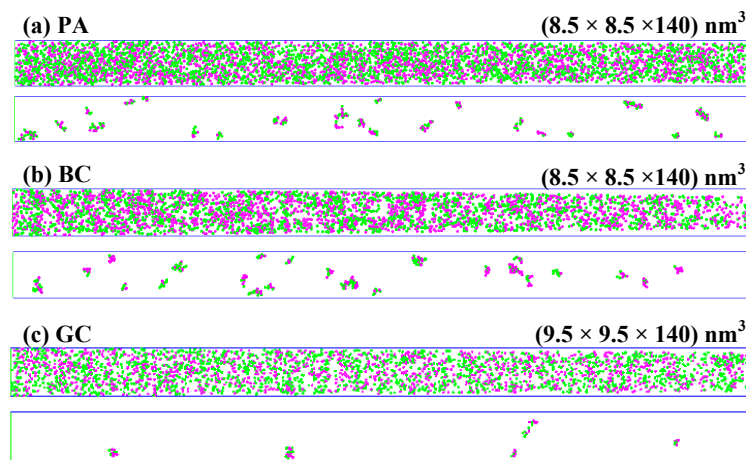


Fig. 2: The distribution of clusters within comparable parts of the reconstructed APT volumes after application of the maximum separation method. (a) PA: directly pre-aged sample, (b) BC: naturally aged sample of high solute content, (c) GC: naturally aged sample of low solute content.

3.2 Quantitative description of clusters

Since this work aims to describe how the solute distribution changes upon ageing, the Al content of the clusters is not addressed. The *radius of gyration of solutes* [8], which is here used as an indicator of the cluster size, is calculated by the following expression:

$$R_g = \sqrt{\frac{\sum_{i=1}^n ((x_i - x_0)^2 + (y_i - y_0)^2 + (z_i - z_0)^2)}{n}} \quad (1)$$

where x_i , y_i and z_i are the coordinates of the i th solute atom in the cluster; x_0 , y_0 and z_0 are the coordinates of the centre of mass of the cluster and n is the number of solute atoms in the cluster. Since atomic masses are taken into account, this quantity does not generally represent the physical extent of a cluster. However, in our case the solute elements have adjacent atomic masses, making R_g a useful indicator of cluster size. The *cluster compactness* is calculated as n/R_g^3 , expressing the number of solute atoms contained within the radius of gyration of solutes.

Figure 3 shows the variation of cluster size and compactness within each dataset. The curves represent the envelopes of histogram distributions and absolute cluster numbers can be obtained by rescaling the percentages with the cluster numbers in Table 2. For all alloy conditions the distributions are uniquely peaked around quite similar mean values, both with regard to compactness and radius of gyration of solutes. However, for the GC alloy a higher fraction of less close-packed clusters, that have on average a higher radius of gyration of solutes, are identified. This is a direct consequence of the higher d_{max} value used for this alloy compared to for the PA and GC alloys.

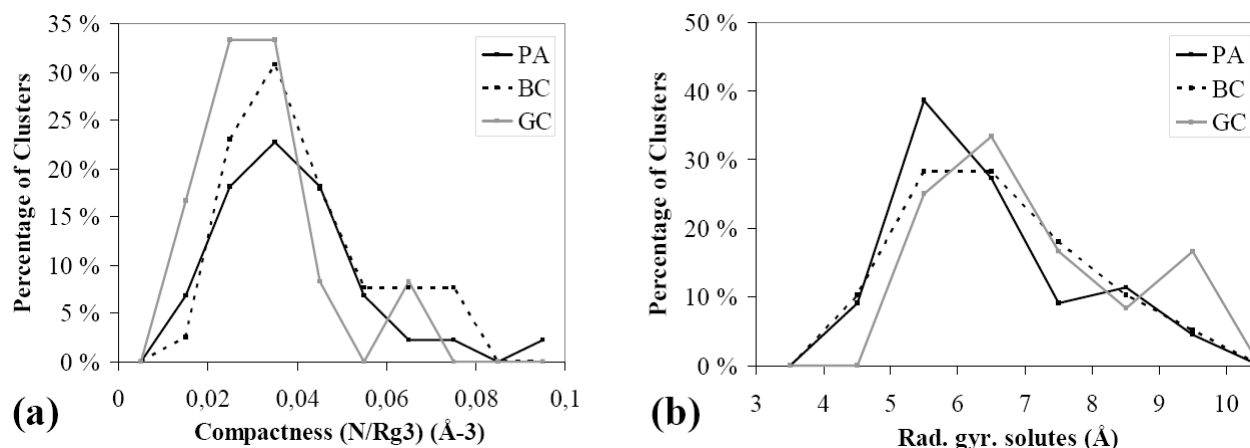


Fig. 3: The envelopes of the histogram distributions for the three alloy conditions in Table 1 of (a) cluster compactness and (b) cluster radius of gyration of solutes.

All the clusters obtained in this study were so-called co-clusters containing both Mg and Si atoms. The compositional variations of the clusters formed in the various samples are visualized in Figure 4. Here we see the envelopes of the histogram distributions of Mg/Si ratios in the clusters. This plot facilitates direct comparison of the atomic content of clusters, and the absolute cluster numbers can be obtained by rescaling the percentages of Figure 4 with the cluster numbers in Table 2. The most prominent feature of Figure 4 is that the compositional distributions corresponding to the PA and GC conditions are very similar. This is interesting since for both these conditions the clusters formed are reported to have a positive effect on subsequent precipitation during artificial ageing [4, 7]. The distributions show a broad, unique, peak centered at an Mg/Si ratio close to 1, implying that a high number of clusters have formed with a composition of approximately Mg₁Si₁. Several experimental studies of well-developed GP-zones, which is the next phase in the precipitation sequence, have reported a composition of approximately Mg₁Si₁ for these [1, 4, 14]. This similarity with regard to composition strongly suggests that the PA and GC clusters can evolve into more developed phases.

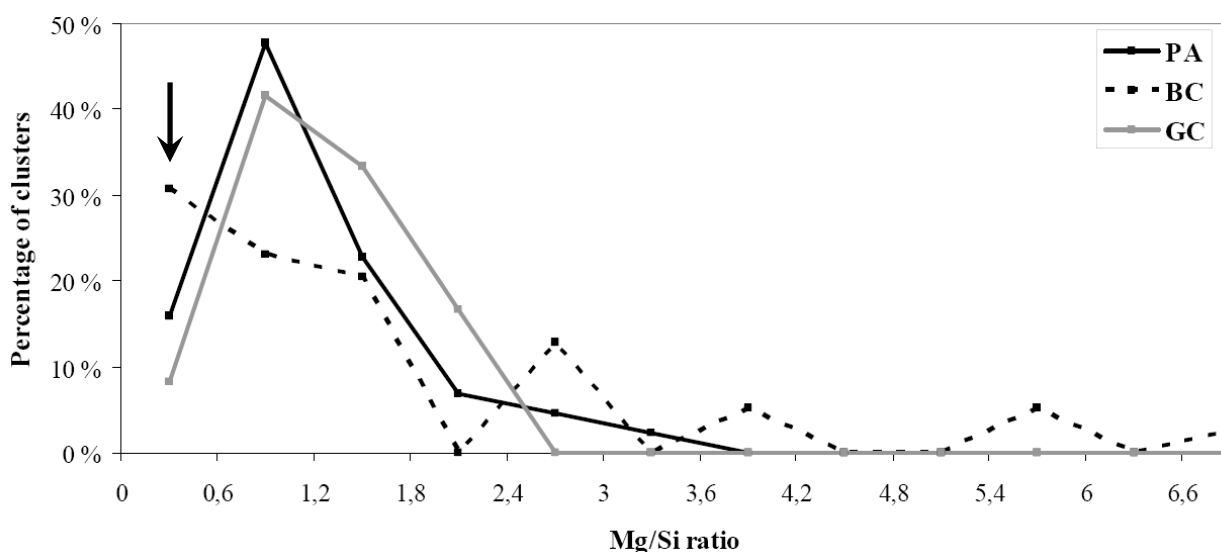


Fig. 4: The envelopes of histogram distributions of the Mg/Si ratios of observed clusters. Both pre-ageing clusters and clusters formed during natural ageing in an alloy of low solute content show a prominent peak around Mg/Si ~1, indicating a high number of clusters containing equal amounts of Mg and Si atoms. The arrow marks a high percentage of clearly Si-rich clusters for the BC alloy.

The distribution of cluster compositions in the BC alloy differs significantly from those of the GC and PA alloys. A broad range of different cluster compositions is seen to form in the BC alloy and a high number of the clusters are clearly Si-rich or clearly Mg-rich. The cluster compositions do not generally match the 1:1 stoichiometry which is reported for the first distinct phase in the precipitation sequence [1, 4, 14], making it likely that a significant proportion of the clusters cannot nucleate more developed precipitates.

4. Conclusion

The clusters produced in Si-rich Al-Mg-Si alloys during direct pre-ageing were compared to those forming during 2 months of natural ageing in similar alloys of high and low solute content. It was found that all investigated alloy conditions produced clusters of similar size and compactness. During direct pre-ageing treatment a high number density of clusters were found to form, most of which had Mg/Si ratios close to 1. In the alloy of low solute content the clusters produced during natural ageing were few, but compositionally equivalent to those forming during direct pre-ageing. As both these conditions show a positive effect on precipitation during subsequent ageing, the clusters with Mg/Si ratios close to 1 are believed to provide nucleation sites for the more developed phases in the precipitation sequence. The alloy of high solute content, on the other hand, produced a high number density of clusters of various compositions. Since most of these do not match the 1:1 stoichiometry of the first distinct phase in the precipitation sequence, they are believed to not provide nucleation sites for more developed phases. This may explain the detrimental effect of intermediate room temperature storage for these alloys.

5. Acknowledgements

This work was financially supported by The Research Council of Norway via two projects: the FRINAT project (Fundamental investigations of solute clustering and precipitation) and the BIP project Kimdanningskontroll (Nucleation Control), which is supported by Norwegian industry: Hydro Aluminium AS, Steertec Raufoss AS.

References

- [1] G. Edwards, K. Stiller, G. Dunlop and M. Couper: *Acta Mater.* 46 (1998) 3893-3904.
- [2] S.J. Andersen, C.D. Marioara, R. Vissers, A.G. Frøseth and H.W. Zandbergen: *Mater. Sci. Eng. A* 444 (2007) 157-169.
- [3] C.D. Marioara, S.J. Andersen, J. Jansen and H.W. Zandbergen: *Acta Mater.* 51 (2003) 789-796.
- [4] M. Murayama and K. Hono: *Acta Mater.* 47 (1999) 1537-1548.
- [5] J. Røyset, T. Stene, J.A. Sæter and O. Reiso: *Mater. Sci. Forum* 519-521 (2006) 239-244.
- [6] K. Yamada, T. Sato and A. Kamio: *Mater. Sci. Forum* 669 (2000) 331-337.
- [7] C.S.T. Chang, I. Wieler, N. Wanderka and J. Banhart: *Ultramicroscopy* 109 (2009) 585-592.
- [8] K. Hono: *Progress in Materials Science* 47 (2002) 621-729.
- [9] M.K. Miller: *Atom Probe Tomography: analysis at the atomic level*, (Kluwer Academic / Plenum Publishers, New York, 2000) pp. 184-189.
- [10] E. Bemont, A. Bostel, M. Bouet, G. Da Costa, S. Chambreland, B. Deconihout and K. Hono: *Ultramicroscopy* 95 (2003) 231-238.
- [11] G. Da Costa, F. Vurpillot, A. Bostel, M. Bouet and B. Deconihout: *Rev. Sci. Instrum.* 76 (2005) 013304.
- [12] F. Danoix, M.K. Miller and A. Bigot: *Ultramicroscopy* 89 (2001) 177.
- [13] L.T. Stephenson, M.P. Moody, P.V. Liddicoat and S.P. Ringer: *Microsc. Microanal.* 13 (2007) 448-463
- [14] M. Murayama, K. Hono, M. Saga and M. Kikuchi: *Mater. Sci. Eng. A* 250 (1998) 127.